TECHNICAL UNIVERSITY OF CLUJ-NAPOCA

ACTA TECHNICA NAPOCENSIS

Series: Applied Mathematics, Mechanics, and Engineering
Vol. 58, Issue II, June, 2015

PLAN MODEL TO ANALYZE THE STATE OF STRESSES AND STRAINS OF THE HUMAN PROXIMAL FEMORAL BONE

Adrian-Ioan BOTEAN, Dan Silviu MÂNDRU, Mihail HĂRDĂU

Abstract: *This study aims to analyze the state of stresses and strains of the human proximal femoral bone using an innovative plan model. Behavior analysis for this plan model is performed experimental, using digital image correlation, and numerically, using finite element method. Mechanical load model is properly to unipodal support.*

Key words: *femoral human bone, plane model, digital image correlation, finite element method*

1. INTRODUCTION

This study aims to evaluate, in terms of quality, state of stresses and strains of the human proximal femoral bone through a plan model using experimental method (digital image correlation) and numerical method (finite element analysis). Starting from the schematization orientation of trabecular tissue structure of the proximal human femoral bone made by various researchers such as von Meyer (1867), Wolff (1886) and Koch (1917) – see figure 1 – and a careful analysis of the structures of a real model by providing a longitudinal section through a human femoral bone (cf. figure 2) has been proposed a new version the schematic of plane model shown in figure 3 [1], [2], [5], [7], [9], [11], [14], [20], [22].

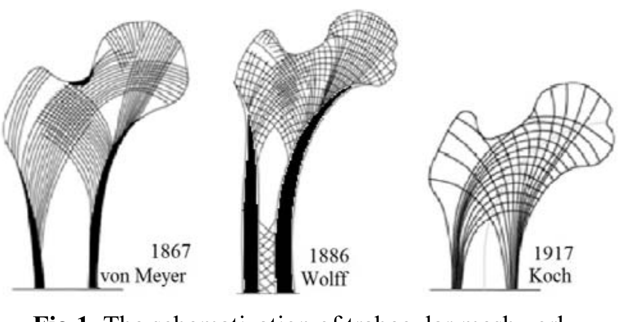

Fig.1. The schematization of trabecular meshwork structure.

Components of trabecular meshwork structure are: the main group of compression, secondary compression group, the main tension group, secondary tension group, the ligamentous group and growth lines. Model plan shows a total of 170 trabeculae (figure 3).

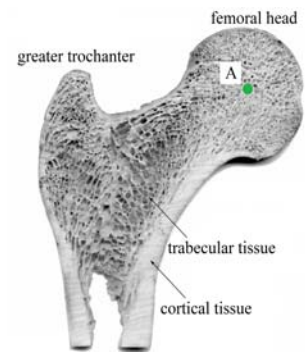

Fig.2. Longitudinal section through a human femoral bone (proximal area).

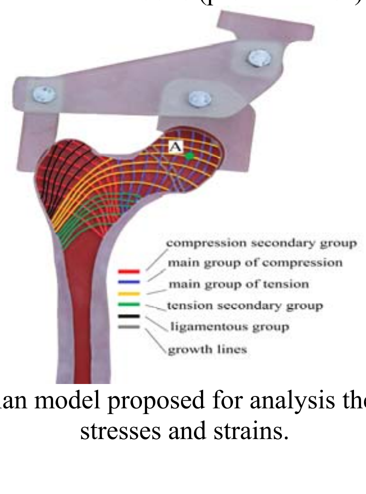

Fig.3. Plan model proposed for analysis the state of stresses and strains.

Fig.4. Physical developed plan model.

Trabecular structure is made of epoxy resin and empty space of this structure is filled with silicone rubber. Mechanical load system is designed to take into account coxo-femoral joint action (femoral neck area) and the action of muscles: middle gluteal (gluteus medius) and lower gluteal (gluteus minimus) – the greater trochanter area – corresponding unipodal support (see figure 3). In unilateral support or unipodal support the hip joint is the point of supporting the entire weight of the human body, thus making unilateral support to be the most dangerous position. Here, the femoral bone is stabilized in acetabulum by the abductor muscle group: gluteal muscle small, medium and large [15].

2. EXPERIMENTAL ANALYSIS

For mechanical loading of plan model is used universal testing machine Instron, model 6631 (cf. figure 5).

Static mechanical loading is done progressivley forces from 1 to 10 N. Load pattern is shown in figure 6. For each force value (1, 2, 3, …, 10 N) defines a path of constant load that lasts 20 seconds, time in which the image acquisition of the plane model shall carry out under load. These images are acquired by Q400 system (Dantec Dynamics), analysis field displacements being made by digital image correlation method with Istra 4D software (see figure 5). It will evaluate in vertical plane the displacement (d_y) of de center of the femoral head, marked by point A [6], [23].

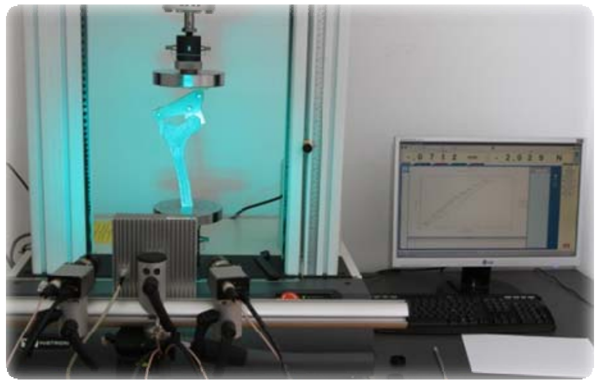

Fig.5. The 2D model loaded by Instron 6631 universal testing machine and analyzed by digital image correlation method (Q400).

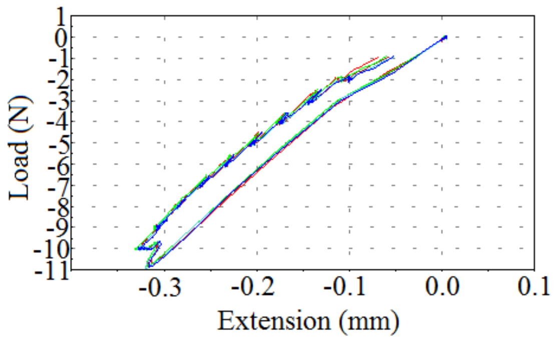

Fig.6. Mechanical load patern of the 2D model.

3. NUMERICAL ANALYSIS

2D numerical model (dimensional identical to that achieved phisycal) is modeled through 1,086 nodes defined in the finite element software RDM 6.15 by the system of chartesian coordinate. Through successive mesh, changing the size of the finite elements (have been used triangular finite elements with six nodes and semi-circular side), the model is composed of a number of 6,877 finite elements (see figure 7).

Trabecular structure is epoxy resin for which elastic modulus (Young's modulus) is 2,200 MPa and transverse contraction coefficient is 0.36. The free spaces of the trabecular meshwork structure are filled with silicone rubber having elastic modulus 8 MPa and traverse contraction coefficient has a value of 0.47. Mechanical load is achieved based load pattern from figure 6 [3], [4], [16], [21], [24].

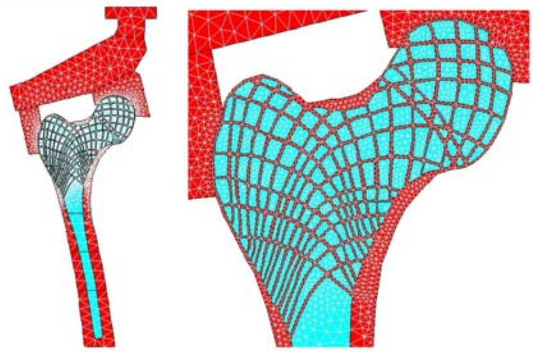

Fig.7. Virtual plane model.

4. COMPARATIVE STUDY

Table 1 and figure 8 summarizes results of the numerical (finite element method - FEA) and experimental (digital image correlation - DIC) on the displacement of the center of the femoral head in relative to vertical plane (d_{yA}) depending on load pattern of the 2D model shown in figure 6. In figure 9 are represented, through iso-colors, field displacements in vertical plane (d_y) obtained by of the two methods of investigation.

Table 1

Comparative analysis of the displacement of the femoral head center (point A).

Nr. crt.	F [N]	DIC d_{yA} [mm]	FEA d_{yA} [mm]	Ab.rel. [%]
1	-10	-0,151	-0,155	2,58
2	-9	-0,139	-0,140	0,71
3	-8	-0,127	-0,124	2,36
4	-7	-0,117	-0,11	5,98
5	-6	-0,103	-0,093	9,7
6	-5	-0,088	-0,081	7,95
7	-4	-0,077	-0,062	19,48
8	-3	-0,058	-0,049	15,51
9	-2	-0,043	-0,031	27,9
10	-1	-0,021	-0,018	14,28

A comparative analysis of the results obtained through the two methods is observed a good convergence deviations ranging in reasonable limits, thus validating the numerical 2D model. The plane model is suitable for carrying out a more detailed study of the state of stresses, using finite element analysis, behavior under mechanical load for proximal area, with reference to the trabecular structure in particular.

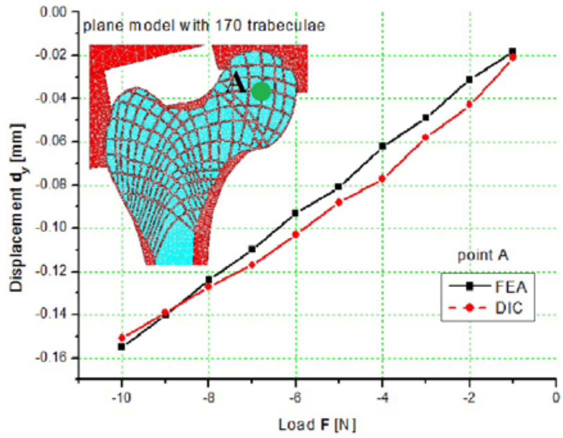

Fig.8. Graph of displacement variation in vertical plane to point A.

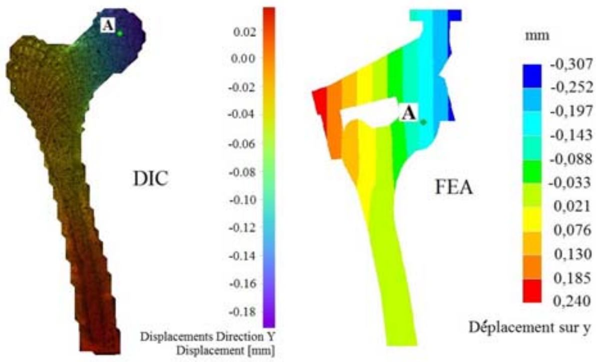

Fig.9. The field of displacements in the vertical plane obtained by DIC and FEA.

As a result of the action mechanical strain forces in the femoral head and the greater trochanter in the elements that compose the structure is generated axial efforts (tensile and compression). Thus, by the finite element analysis can be shown, through iso-colors, state of stresses identifying the maximum loaded area. To characterize this state of stresses in figure 10 is shown, through iso-colors, Tresca equivalent stress distribution, in figure 11 maximum principal stress distribution, in figure 12 minimum principal stress distribution. Are summarized in table 2 Tresca equivalent stress values and the maximum and minimum principal stresses depending on application force F.

From figure 10 it can be seen as trabecular structure takes over mechanical load and is distributed to cortical structure and especially toward diaphysis where the maximum stress is registered, the critical area – femoral neck – thus subjected to a lower load level. It is noted as the imported role that it plays trabecular structure and integrity of this structure depends on the integrity of the structure of human femoral bone (proximal area). Maximum principal stresses (Sigma YY), represented in figure 11, shows how the main compression group and secondary compression group (see figure 3) register a higher level of load that the main tension group and secondary tension group (see figure 12), the maximum level of stress is in small trochanter area respectively in diaphysis area. This area has a high capacity to take over the compressive stresses. Minimum principal stresses (Sigma xx), shown in figure 12, emphasizes that main tension group and secondary tension group have a maximum level of load in posterior area of proximal structure. Noteworthy is the fact that growth lines (see figure 3) takes over the tension efforts. In figure 13 is the graph of variation of Tresca equivalent stress well as the maximum principal stress (Sigma YY) and minimum principal stress (Sigma xx) depending on application force F drawn from the data in table 2.

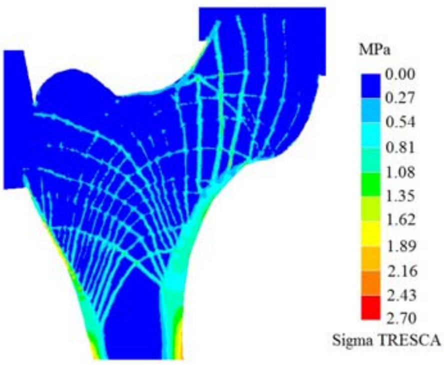

Fig.10. Tresca equivalent stress distribution.

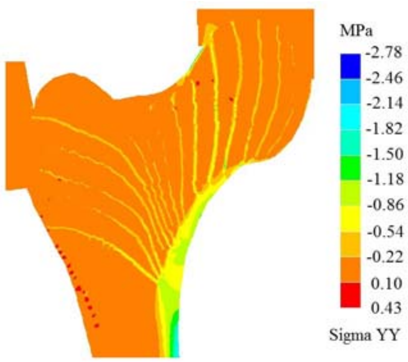

Fig.11. Maximum principal stress distribution.

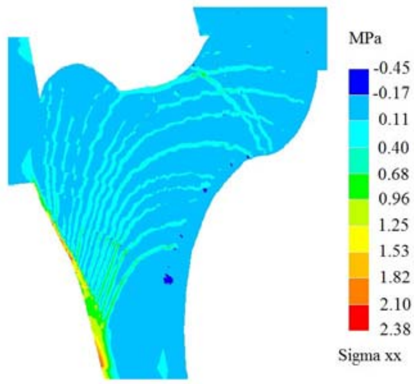

Fig.12. Minimum principal stress distribution.

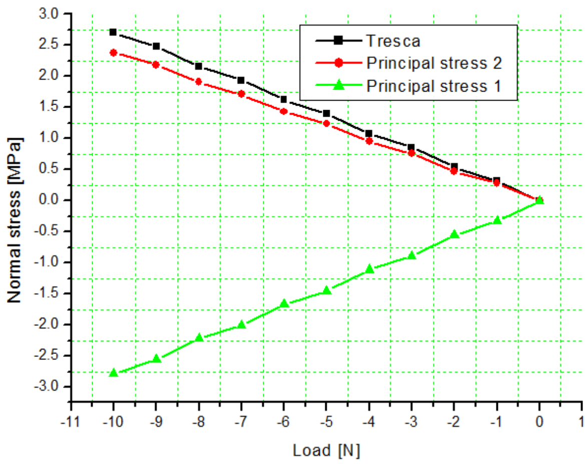

Fig.13. The graph of variation of Tresca equivalent stress, the maximum principal stress (Sigma YY) and minimum principal stress (Sigma xx) depending on application force F drawn from the data in Table 2.

Table 2

The value of Tresca equivalent stress, the maximum principal stress (Sigma YY) and minimum principal stress (Sigma xx) depending on application force F.

Nr. crt.	F [N]	Tresca [MPa]	SYY (σ_1) [MPa]	Sxx (σ_2) [MPa]
1	-10	2.70	-2.78	2.38
2	-9	2.48	-2.56	2.19
3	-8	2.16	-2.22	1.91
4	-7	1.94	-2.00	1.71
5	-6	1.62	-1.67	1.43
6	-5	1.40	-1.45	1.24
7	-4	1.08	-1.11	0.95
8	-3	0.86	-0.89	0.76
9	-2	0.54	-0.55	047
10	-1	0.32	-0.33	0.28

5. CONCLUSIONS

By analyzing the graphical representation of figure 8 and table 1 show that the relative deviations between the two sets of results validate the proposed 2D model. Thus, based on this two-dimensional model can be analyzed states of stress and strain in the femoral neck, extensive attention being paid to the trabecular structure. On the basis of figure 10 can highlight de maximum load of proximal area namely the small trochanter. Figure 11 and figure 12 highlights the maximum and minimum principal stress distribution and the tension and compression lines take the mechanical loading – appropriate loading unipodal support.

It can be concluded that the spongy (trabecular) tissue provides maximum strength using a minimum of trabecular material, which is distributed by mechanical load directions, in the longitudinal plane orientation of the trabecular bone being after the main stress directions.

The proposed 2D model comprises a group of 14 tension lines, a group of 15 compression lines and the two lines which form the growth zone. Thus, based on this plane model can be analyzed states of stress and strain in the femoral neck in some special situations: proximal area present failures distribution of trabecular structure (osteoporosis) or fracture – a case in which can be modeled different osteosynthesis systems [10], [12], [13], [17], [18], [19], [25].

6. ACKNOWLEDGEMENTS

This work was possible with the financial support of the Sectorial Operational Program for Human Resources Development, co-financed by the European Social Found, under the project number PSDRU/159 /1.5/S/137516 with the title “Inter-University Partnership for Excellence in Engineering - PARTING”.

7. BIBILOGRAFIE

[1] Baciu C. *Aparatul locomotor. Anatomie funcțională, biomecanică, semiologie clinică, diagnostic diferențial*, 1981.

[2] Beaupied H., Lespessailles E., Benhamou C.L., *Evaluation of macrostructural bone biomechanics*, Joint Bone Spine, Volume 74, Issue 3, 2007.

[3] Bessho M., Ohnishi I., Matsuyama J., Matsumoto T., Imai K., Nakamura K., *Prediction of strength and strain of the proximal femur by a CT-based finite element method*, Journal of Biomechanics, Volume 40, 2007.

[4] Bessho M., Ohnishi I., Matsumoto T., Ohashi S., Matsuyama J., Tobita K., Kaneko M., Nakamura K., *Prediction of proximal femur strength using a CT-based nonlinear finite element method: Diferences in predicted fracture load and site with changing load and boundary conditions*, Bone, Volume 45, 2009.

[5] Botean A.I., Takacs I.A., *The study of massive trochanterion fractures*, Meditech, Cluj-Napoca, 2011.

[6] Dickinson A.S., Taylor A.C., Ozturk H., *Experimental validation of a finite element model of the proximal femur using digital image correlation and a composite bone model*, Journal of Biomechanical Engineering, vol.133, no. 1, 2010.

[7] Gibson L.J., Ashby M.F., *Cellular solids. Structure and properties – Second edition*, 2001.

[8] Gregory J.S., Aspden R.M., *Femoral geometry as a risk for osteoporotic hip fracture in men and women*, Medical Engineering & Physics, Volume 30, Issue 10, 2008.

[9] Griffith J.F., Genant H.K., *Bone mass and arhitecture determination: state of the art*, Best practice & Research Clinical Endocrinology & Metabolism, Vol. 22, No. 5, 2008.

[10] Gupta H.S., Zioupos P., *Fracture of bone tissue: The ‘hows’ and the ‘whys’*, Medical Engineering & Physics, Volume 30, 2008.

[11] Griffith J.F., Genant H.K., *New Imaging Modalities in Bone*, Curr Rheumatol Rep, Volume 13, 2011.

[12] Holroyd C., Cooper C., Dennison E., *Epidemiology of osteoporosis*, Best practice & Research Clinical Endocrinology & Metabolism, Vol. 22, No. 5, 2008.

[13] Ito M., Wakao N., Hida T., Matsui Y., Abe Y., Aoyagi K., Uetani M., Harada A., *Analysis of hip geometry by clinical CT for the assessment of hip fracture risk in elderly Japanese women*, Bone, Volume 46, Issue 2, 2010.

[14] Ito M., Nakata T., Nishida A., Uetani M., *Age-related changes in bone density, geometry*

and biomechanical properties of the proximal femur: CT-based 3D hip structure analysis in normal postmenopausal women, Bone, Volume 48, 2011.

[15] Kamina P., *Atlas de anatomie. Morfologie. Funcționare. Aspecte clinice*, 2014.

[16] Langton C.M., Pisharody S., Keyak J.H., *Comparison of 3D finite element analysis derived stiffness and BMD to determine the failure load of the excised proximal femur*, Medical Engineering & Physics, Volume 31, 2009.

[17] Li W., Kornak J., Harris T., Keyak J., Li C., Lu Y., Cheng X., Lang T., *Identify fracture-critical regions inside the proximal femur using statistical parametric mapping*, Bone, Volume 44, 2009.

[18] Li W., Kornak J., Harris T., Keyak J., Li C., Lu Y., Cheng X., Lang T., *Bone fracture risk estimation based on image similarity*, Bone, Volume 45, 2009.

[19] Little J.P., Taddei F., Viceconti M., Murray D.W., Gill H.S., *Changes in femur stress after hip resurfacing arthroplasty: Response to physiological loads*, Clinical Biomechanics, Volume 22, 2007.

[20] Philips, A.T.M., *Structural Optimisation: Biomechanics of the Femur*, Engineering and Computational Mechanics, Vol. 165, 2012.

[21] Ramos A., Simoes J.A., *Tetrahedral versus hexahedral finite elements in numerical modelling of the proximal femur*, Medical Engineering & Physics, Volume 28, 2006.

[22] Rho J.Y., Kuhn-Spearing L., Zioupos P., *Mechanical properties and the hierarchical structure of bone*, Medical Engineering & Physics, Volume 20, Issue 2, 1998.

[23] Sciammarella C.A., Sciammarella F.M., *Experimental Mechanics of Solids*, 2012.

[24] Yosibash Z., Trabelsi N., Milgrom C., *Reliable simulations of the human proximal femur by high-order finite element analysis validated by experimental observations*, Journal of Biomechanics, Volume 40, 2007.

[25] Zioupos P., Gresle M., Winwood K., *Fatigue strength of human cortical bone: Age, physical, and material heterogeneity effects*, Journal of Biomedical Materials Research Part A, Volume 86A, Issue 3, 2007.

Model plan pentru analiza stării de tensiuni şi deformații din zona proximală a osului femural uman

Rezumat: *Prezentul studiu îşi propune analiza stărilor de tensiuni şi deformații din zona proximală a osului femural uman pe baza unui model plan inovativ. Analiza comportamentului modelului bidimensional este efectuată experimental, utilizând metoda corelației digitale a imaginii, şi numeric, utilizând metoda elementului finit. Modelul de solicitare mecanic este corespunzător unui sprijin unipodal.*

Adrian Ioan BOTEAN, Lecturer, Ph.D., Technical University of Cluj-Napoca, Department of Mechanical Engineering, 103-105 Muncii Blvd., 400641, Cluj-Napoca, +40-264-401751, Adrian.Ioan.Botean@rezi.utcluj.ro.

Dan Silviu MÂNDRU, Prof., Ph.D., Technical University of Cluj-Napoca, Department of Mechatronics and Machine Dynamics, 103-105 Muncii Blvd., 400641, Cluj-Napoca, +40-264-401602, dan.mandru@mdm.utcluj.ro.

Mihail HĂRDĂU, Prof., Ph.D., Technical University of Cluj-Napoca, Department of Mechanical Engineering, 103-105 Muncii Blvd., 400641, Cluj-Napoca, +40-264-401608, mihailhărdău@yahoo.com.